CHARACTERIZATION AND SIMULATIONS OF ELECTRON BEAMS PRODUCED FROM LINAC-BASED INTENSE THz RADIATION SOURCE

N. Chaisueb†, N. Kangrang, S. Rimjaem, J. Saisut, Plasma and Beam Physics Research Facility, Department of Physics and Materials Science, Faculty of Science, Chiang Mai University, Chiang Mai 50200, Thailand

Abstract

Electron beams with a maximum kinetic energy of around 2.5 MeV and a macropulse current of about 1 A are produced from an S-band thermionic cathode RF-gun of the linear accelerator system at the Plasma and Beam Physics (PBP) Research Facility, Chiang Mai University (CMU), Thailand. An RF rectangular waveguide input-port and a side coupling cavity of the PBP-CMU RF gun introduce asymmetric electromagnetic field distribution inside the gun cavities. To investigate the effect of the asymmetric field distribution on electron beam production and acceleration, measurements and simulations of the electron beam properties were performed. In this study we use well calibrated current transformers, alpha magnet energy slits, and a Michelson interferometer to measure the electron pulse current, the beam energy, and the bunch length, respectively. This paper presents the measurement data of the electron beam properties at various location along the beam transport line and compares the results with the beam dynamic simulations by using the particle tracking program ELEGANT. Moreover, the RF field feature and the cathode power were optimized in order to achieve the high qualities of the electron beam produced from the RF gun. This result implies and correlates to the electron back-bombardment effect inside the gun cavities.

INTRODUCTION

The electron linear accelerator at the Plasma and Beam Physics Research Facility (PBP-CMU Linac), Chiang Mai University, Thailand, is used to generate short electron bunches for generation of intense coherent THz radiation in forms of transition radiation and undulator radiation [1-4]. The PBP-CMU Linac transport line consists of two main parts that are the Gun-to-Linac (GTL) section and the Linac-to-Experimental station (LTE) section. In the GTL section, electron bunches are produced from a thermionic RF-gun and are transported to an alpha magnet by using three quadrupoles and two pairs of steering magnets to focus and guide the beam to centre of the alpha magnet entrance.

The alpha magnet is used as a magnetic bunch compressor and also as an energy measuring instrument by utilizing high and low energy slits installed inside its vacuum chamber. Furthermore, the energy slits are used to filter out low energy electrons in order to decrease the energy spread before the beam is post-accelerated in an S-band travelling-wave linear accelerator (linac) structure. In the LTE section, relativistic electron bunches exiting from the post-accelerated linac are currently used to generate the coherent THz radiation at the transition radiation station. To measure the electron beam energy after the linac acceleration, the beam is guided through a 60^{o} dipole magnet and a beam dump equipped with a Faraday cup at the end of the beam transport line.

Various beam diagnostic instruments are installed along the PBP-CMU Linac system to measure and analyse electron beam properties. Firstly, the current and pulse length of the electron macropulse were monitored with a non-destructive device called a current transformer. This device consists of a ferrite-core toroid with a ceramic tube enclosing the electron beam path and a loaded resistor. Secondly, the electron beam energy and energy spread were measured by using the alpha magnet energy slits and the current transformer for the beam after the RF-gun acceleration and a combination of a dipole magnet, a view screen, and a Faraday cup for the beam after the linac acceleration. Thirdly, a screen station, which consists of a phosphor screen and a CCD camera, is used to capture the transverse distribution of the electron beam. The beam image is then analysed with MATLAB code to obtain the transverse size and profile. Lastly, the bunch length measurement is performed by using an autocorrelation technique with a Michelson interferometer and a pyroelectric detector.

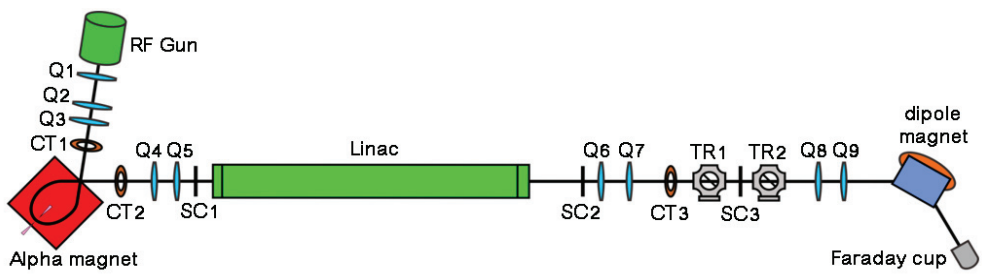

Figure 1: Schematic setup of the PBP-CMU linac system and the beam transport line. The letters Q, CT, SC and TR represent quadrupole magnets, current transformers, screen stations and transition radiation stations.

† Corresponding author: natthawut_chai@cmu.ac.th

ISBN 978-3-95450-177-9

GUN-TO-LINAC

Experimental Results

The electron beam performance in the Gun-to-Linac (GTL) section corresponds significantly to the RF-field feature inside the RF-gun such as RF pulse length, RF power, and RF waveform. When the RF pulse length is longer, the RF peak power gets higher and the flat top of waveform is longer due to the imperfection of the RF pulse production and power amplification. The RF pulse length of the PBP-CMU RF-gun can be varied up to 8 μs (FWHM). However, the long RF pulse is avoided since the effect of electron back-bombardment is large, which is a well-known disadvantage of the thermionic RF-gun. This effect leads to instability of the beam output, breakdown of the RF-gun operation and reduction of the electron energy gain due to the beam loading effect. The RF pulse length of 2.8 μs FWHM with the forward power of 3.65 MW at the proper gun temperature of 27ºC was used for the experiments presented in this paper in order to minimize the dark current and the electron back-bombardment effect.

After the electron beam exits the RF gun, a macropulse current is measured at the first current transformer (CT1) with the maximum macropulse current of about 1 A (as shown in Fig. 2). The electron macropulse has a triangular-like pulse shape with a FWHM pulse width of around 1-2.5 μs depending on the cathode temperature. A fraction of low energy electrons is filtered out with the low energy slit in the alpha magnet vacuum chamber. About 30% of the beam with high energy electrons exits the alpha magnet and is observed at the second current transformer (CT2) with the maximum macropulse current of about 0.35 A.

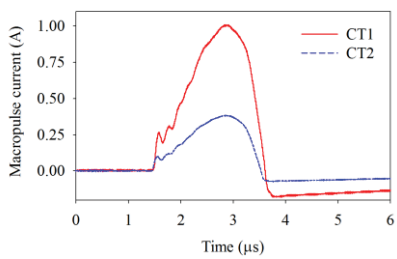

Figure 2: Electron macropulse currents at the gun exit (CT1) and at the exit of the alpha magnet (CT2).

The dependence of electron charge on the cathode temperature for different RF powers is shown in Fig. 3. It illustrates that electrons started to emit from the cathode at lower cathode temperature, when higher RF power was used. This indicates the more effect of the electron back-bombardment at higher RF power. For all RF powers, the number of electrons is low at high cathode temperature due to the back-bombardment phenomena.

The electron macropulse current, pulse width and maximum kinetic energy were measured at various cathode powers by using the current transformer CT1 and the alpha magnet energy slits. The measurement results at the RF peak power of 3.65 MW are plotted in Fig. 4 and Fig. 5. According the experimental results, electrons start to emit from the cathode when the cathode power is above 13 W. The maximum kinetic energy and the beam pulse width decrease quickly when the cathode power above 13.2 W. For the cathode power in the range of 13.2 W to 16.5 W, the beam energy reduces from 2.6 MeV to 0.5 MeV and the beam pulse width shortens from 2.8 μs to 1 μs. Contradictory, at these cathode powers the beam pulse current increases immediately up to 1 A and then decreases gradually to about 0.9 A when the cathode power is higher than 14.2 W. This is clearly due to the result of back-bombardment effect.

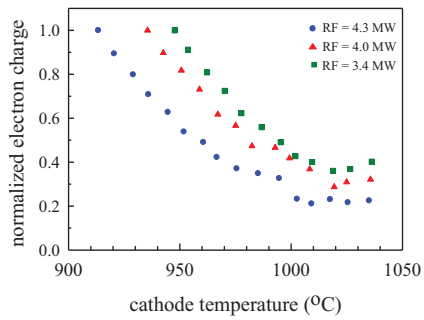

Figure 3: Normalized electron charge at the gun exit as a function of cathode temperature for three RF powers.

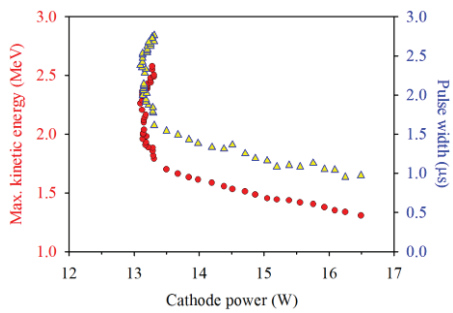

Figure 4: Maximum kinetic energy (dots) and pulse width (triangles) of electron beam as a function of cathode power.

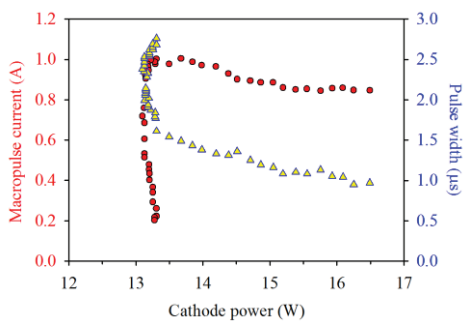

Figure 5: Electron macropulse current (dots) and macropulse width (triangles) as a function of cathode power.

The alpha magnet energy slits were used to measure the energy spectrum of electron beams produced from the RF-gun for three different cathode temperatures; 945, 950 and 960ºC. The experimental results are shown in Fig. 6. For the temperature of 950ºC, the integrated charge is higher than other two temperatures. Furthermore, the main part of electrons has more uniform energy in the high energy range with the maximum charge per energy

ISBN 978-3-95450-177-9

bin. Therefore, the cathode temperature of 950ºC is the most optimal condition for electron production. Experimental experience also showed that the RF-gun had stable operation at this temperature.

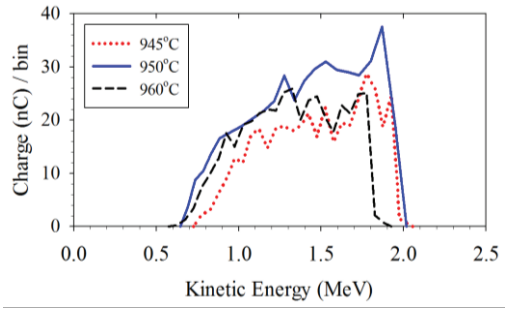

Figure 6: Energy spectra of electron beams produced at the cathode temperatures of 945, 950 and 960ºC.

The transverse image of electron beam with the maximum total energy of around 2.5 MeV was measured prior the linac entrance at the screen station SC1, which can be used to analyze the transverse intensity distribution and the transverse beam size as shown in Fig. 7. Both horizontal and vertical beam profiles were fitted with a Gaussian distribution. The results show that the horizontal and vertical beam sizes are 3.1 mm and 3.4 mm, respectively.

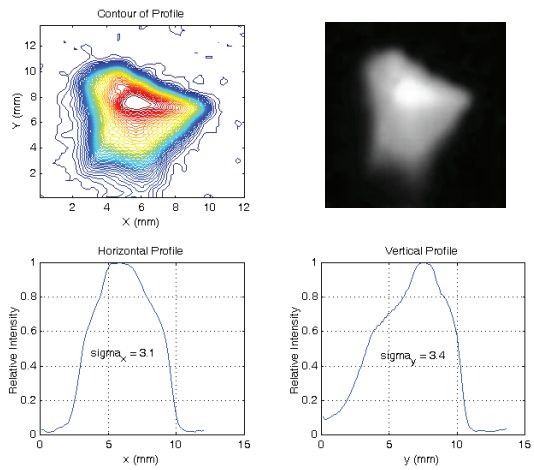

Figure 7: Intensity contour, beam image and relative horizontal and vertical beam profiles for the 2.5 MeV electron beam measured at the screen station SC1.

Simulation Results

The electron beam dynamic simulation inside the RF-gun was done by using the code PARMELA [5] and the results were reported in [6]. In this study, the particle tracking program ELEGANT [7] was used to investigate the electrons' motion along the beam transport line from the gun exit to the experimental station. Electron beam transverse distributions at different positions in the GTL section are shown in Fig. 8. The electron bunch exits the RF-gun with off-axis centroid position on both horizontal and vertical axes, which is the result of the asymmetric electromagnetic field distribution inside the gun cavities.

As discussed in [6], the electron bunch produced from the RF-gun with asymmetric field distribution has larger emittance value than the electron bunch produced from the symmetric RF-gun. This leads to the increase of the electron transverse size and the off-axis distance from the reference trajectory when the electron bunch arrives the entrance of the alpha magnet as shown in Fig. 8 (b). The steering magnets were used to guide the beam to enter the centroid of the alpha magnet entrance. The electron beam downstream the alpha magnet has smaller beam size in y-axis, which indicates that the alpha magnet has the focusing property in vertical direction. Then, the electron bunch was focused with the quadrupoles before traveling to the linac.

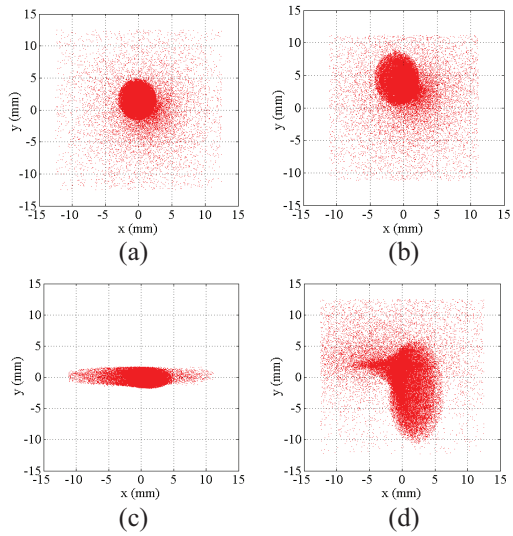

Figure 8: Beam transverse distributions at (a) the gun exit, (b) upstream the alpha magnet, (c) downstream the alpha magnet, and (d) the linac entrance.

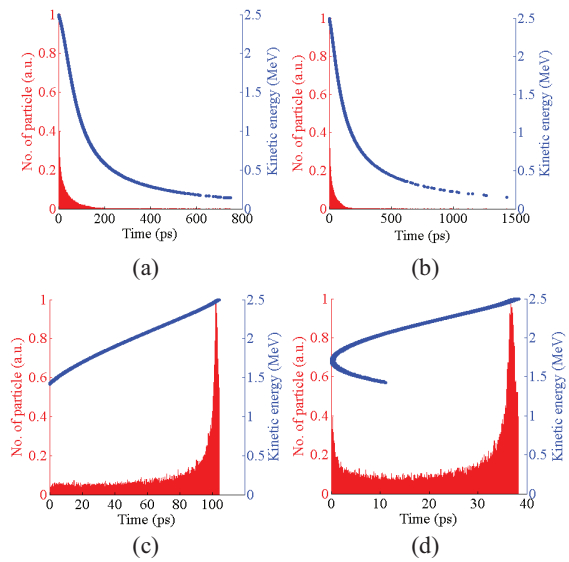

Figure 9: Longitudinal particle distributions at (a) the gun exit, (b) upstream the alpha magnet, (c) downstream the alpha magnet, and (d) the linac entrance.

The longitudinal distributions of the electron bunch at different locations in the GTL section are shown in Fig. 9.

ISBN 978-3-95450-177-9

In this study, the maximum kinetic energy and average energy of electron bunch are 2.5 MeV and 2.2 MeV, respectively. After exiting the RF-gun, the high energy electrons move to the alpha magnet before the low energy ones. When the electrons depart from the alpha magnet, the low energy electrons are in the head of the bunch leading to the bunch compression. The FWHM length of the electron bunch at the alpha magnet exit is about 10 ps compared to about 100 ps at the gun exit. The main fraction of electrons at the linac entrance has the FWHM bunch length of about 3 ps.

LINAC-TO-EXPERIMENTAL STATION

The electron beam with a kinetic energy range of 1.42 to 2.5 MeV was selected by using the energy slits before transporting it to the linac. The beam with a macropulse current of 350 mA and a pulse width of 1.3 μs was measured at CT2. The performance of the linac acceleration involves an input RF power and RF phase, which were optimized to obtain electron beam with maximum energy gain and minimum energy spread. The beam macropulse current after the linac acceleration measured at CT3 was 150 mA with a pulse width of 0.8 μs.

The energy spectrum of the beam measured with the dipole magnet and the Faraday cup in Fig. 10 reveals that the average electron beam energy is 9.8 MeV with energy spread of about 1.08 MeV. Therefore, the energy gain from accelerating in the linac was 7.3 MeV resulting in the linac acceleration gradient of 2.4 MeV/m. The result of the electron bunch length measurement with Michelson interferometer implies that the FWHM length of the electron bunch is calculated to be 124 μm [8].

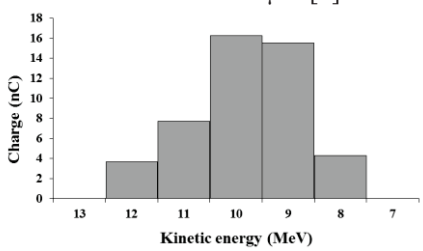

Figure 10: Energy spectrum of the electron beam after the linac acceleration.

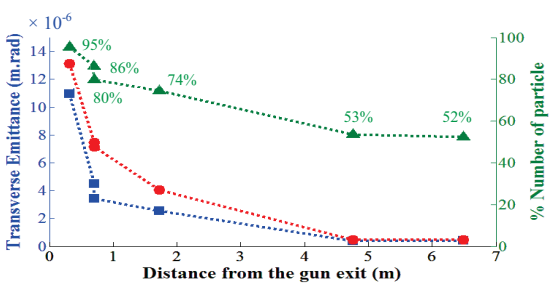

Figure 11: Transverse emittances in x axis (squares) and y axis (dots) with percentage of particle number (triangles) along the PBP-CMU beamline.

Simulation results from program ELEGENT in Fig. 11 and Table 1 suggest that at the experimental station the electron beam with a bunch charge of 27 pC has the geometric emittance of 0.43 mm.mrad.

Table 1: Simulated Electron Beam Properties at the Experimental Station

Parameters	Value
x/y beam size	4.52 / 4.67 mm
x/y emittance	0.41 / 0.45 mm.mrad
Average energy	9.82 MeV
Energy spread	0.24 MeV

CONCLUSION

The RF characteristics and the cathode temperature are the most important parameters for electron beam production of the thermionic RF gun. The effect of the electron back-bombardment is a limitation of the thermionic RF-gun, which affects the macropulse current, the pulse length, and the kinetic energy of the electron beam. The cathode power of around 13.2 W or equivalent to the cathode temperature of 950ºC is the optimal condition for achieving the electron pulses of 2.0-2.5 μs with the maximum energy of 2.0-2.5 MeV and the beam pulse current of 1 A at the gun exit. The simulation results show that the transverse emittance decreases, when the electron bunch arrives at the experimental station. This is the result of the increase of the beam energy and the loss of electrons. The beam emittance will be measured in the future by using the multi-quadrupole scan technique to compare with the simulated result.

ACKNOWLEDGEMENTS

The authors would like to acknowledge the supports by the Department of Physics and Materials Science, the Faculty of Science, Chiang Mai University, the CMU Junior Research Fellowship Program, the Science Achievement Scholarship of Thailand and the Thailand Center of Excellence in Physics (ThEP Center).

REFERENCES

[1] S. Rimjaem *et al.*, "Femtosecond Electron Bunches from an RF-gun", *Nucl. Instr. Meth.*, vol. 533, pp. 62-75, 2004.

[2] C. Thongbai *et al.*, "Femtosecond Electron Bunches, Source and Characterization", *Nucl. Instr. Meth.*, vol. 587, pp. 258-269, 2006.

[3] N. Chaisueb, S. Rimjaem, "Study on undulator radiation from femtosecond electron bunches", in *Proc. 37th Int. Free-Electron Laser Conf. (FEL'15)*, Daejeon, Korea, Aug. 2015, paper WEP062, pp. 702-706.

[4] N. Chaisueb *et al.*, "Optimization of electron beam properties for generation of coherent THz undulator radiation at PBP-CMU linac laboratory", in *Proc. 7th Int. Particle Accelerator Conf. (IPAC'16)*, Busan, Korea, May. 2016, paper TUPOW026, pp. 1803-1805.

[5] L.M. Young, J. H. Billen, "PARMELA", Los Alamos, NewMexico, USA, Los Alamos National Laboratory TechnicalNote LA-UR-96-1835, 2002.

[6] S. Rimjaem *et al.*, "RF study and 3-D simulations of a sidecoupling thermionic RF-gun", *Nucl. Instr. Meth. A*, vol. 736, pp. 10–21, 2014.

[7] ELEGANT, `http://www.aps.anl.gov`

[8] J. Saisut *et al.*, "Construction of the magnetic bunch compressor", *Nucl. Instr. Meth.*, vol. 637, pp. 99-106, 2011

ISBN 978-3-95450-177-9